Electrophysiological abnormalities and arrhythmias in alpha MHC mutant familial hypertrophic cardiomyopathy mice.

C I Berul, … , J G Seidman, M E Mendelsohn

J Clin Invest. 1997;99(4):570-576. https://doi.org/10.1172/JCI119197.

Research Article

A new mouse cardiac electrophysiology method was used to study mice harboring an alpha-myosin heavy chain Arg403Gln missense mutation (alpha-MHC403/+), which results in histological and hemodynamic abnormalities characteristic of familial hypertrophic cardiomyopathy (FHC) and sudden death of uncertain etiology during exercise. Wild-type animals had completely normal cardiac electrophysiology. In contrast, FHC mice demonstrated (a) electrocardiographic abnormalities including prolonged repolarization intervals and rightward axis; (b) electrophysiological abnormalities including heterogeneous ventricular conduction properties and prolonged sinus node recovery time; and (c) inducible ventricular ectopy. These data identify distinct electrophysiologic abnormalities in FHC mice with a specific alpha-myosin mutation, and also validate a novel method to explore in vivo the relationship between specific genotypes and their electrophysiologic phenotypes.

Electrophysiological Abnormalities and Arrhythmias in αMHC Mutant Familial Hypertrophic Cardiomyopathy Mice

Charles I. Berul,*§ Michael E. Christe,‖ Mark J. Aronovitz,‡§ Christine E. Seidman,‖ J.G. Seidman,‖ and Michael E. Mendelsohn‡§
**Division of Pediatric Cardiology, ‡Division of Cardiology, and §The Molecular Cardiology Research Center, New England Medical Center, Tufts University School of Medicine, and the ‖Howard Hughes Medical Institute, Harvard Medical School, Boston, Massachusetts 02111*

Abstract

A new mouse cardiac electrophysiology method was used to study mice harboring an α-myosin heavy chain Arg403Gln missense mutation (α-MHC$^{403/+}$), which results in histological and hemodynamic abnormalities characteristic of familial hypertrophic cardiomyopathy (FHC) and sudden death of uncertain etiology during exercise. Wild-type animals had completely normal cardiac electrophysiology. In contrast, FHC mice demonstrated (*a*) electrocardiographic abnormalities including prolonged repolarization intervals and rightward axis; (*b*) electrophysiological abnormalities including heterogeneous ventricular conduction properties and prolonged sinus node recovery time; and (*c*) inducible ventricular ectopy. These data identify distinct electrophysiologic abnormalities in FHC mice with a specific α-myosin mutation, and also validate a novel method to explore in vivo the relationship between specific genotypes and their electrophysiologic phenotypes. (*J. Clin. Invest.* 1997. 99: 570–576.) Key words: cardiomyopathy • hypertrophy • electrophysiology • disease models, animals • drug screening • hereditary diseases

Introduction

Genetically engineered animal models hold promise for understanding the pathophysiology of mutations that cause human diseases (1, 2). Familial hypertrophic cardiomyopathy (FHC),[1] an inherited cardiovascular disorder characterized in humans by ventricular hypertrophy, arrhythmias, and sudden death, results from mutations in the cardiac myosin gene and other genes of the contractile apparatus (for reviews see references 3 and 4). The human FHC cardiac myosin heavy chain gene mutation Arg^{403}Gln has been engineered into the mouse genome to create a murine model of FHC (5). Homozygous mice (αMHC$^{403/403}$) die within a week after birth, while the heterozygous αMHC$^{403/+}$ mice display both histological and hemodynamic abnormalities characteristic of FHC (5). In addition, the FHC mice demonstrate gender and developmental differences. Male FHC mice demonstrate more severe myocyte hypertrophy, disarray, and interstitial fibrosis than their female littermates, and both sexes show increasing cardiac dysfunction and histopathology as they age. Heterozygous FHC mice also have sudden death of uncertain etiology, especially during periods of exercise (5).

To assess directly the role of individual gene products in in vivo cardiac conduction and to explore the molecular basis of cardiac conduction in normal physiology and disease, we developed a method for cardiac electrophysiology (EP) testing in the mouse (6). Based on clinical protocols used to evaluate cardiac conduction in humans, the method allows assessment of the conduction characteristics of the murine heart in normal and transgenic animals, including evaluation of responses to programmed stimulation and pharmacologic agents. We now report electrophysiologic characterization of αMHC$^{403/+}$ mice, and can identify abnormal cardiac conduction and ventricular arrhythmias in this murine model of a human disease.

Methods

In the present study, complete electrocardiographic and electrophysiological characteristics of fully grown adult (30 wk old) male mice were studied. 11 FHC mice were compared with 13 age- and weight-matched littermate wild-type controls in a prospective, blinded fashion. Electrocardiograph (ECG) data were obtained and correlated with a full electrophysiological (EP) study for each animal, including electrophysiological responses both to programmed stimulation and intravenous isoproterenol infusion. The in vivo mouse protocol for electrophysiological testing has been described in detail (6).

Animals. Male mice (strain 129/BS), weighing 35–57 g each were evaluated. The animals were maintained on Regular Rodent Chow (PROLAB, Syracuse, NY), and allowed free access to food and water. Mice were housed four per cage at 24°C in a facility with 12-h light/dark cycles, in full compliance with the American Association for the Accreditation of Laboratory Animal Care. Approval of the Institutional Animal Care and Use Committee was obtained.

Preoperative preparation. For each study, an animal was anesthetized with a mixture of pentobarbital and ketamine (0.033 mg/g each) given intraperitoneally. The mice were intubated and mechanically ventilated, using a rodent respirator (6). A surface 12-lead elec-

Address correspondence to Charles I. Berul, M.D., Molecular Cardiology Research Center, New England Medical Center, 750 Washington Street, Box 80, Boston, MA 02111. Phone: 617-636-4880; FAX: 617-636-1444; E-mail: charles.berul@es.nemc.org

Received for publication 13 September 1996 and accepted in revised form 5 December 1996.

1. *Abbreviations used in this paper:* A-V, atrioventricular; CSNRT, rate-corrected sinus node recovery time; EP, electrophysiology; FHC, familial hypertrophic cardiomyopathy; LV, left ventricle, RV, right ventricle; SCL, sinus cycle length; SNRT, sinus node recovery time.

J. Clin. Invest.

0021-9738/97/02/0570/07 $2.00
Volume 99, Number 4, February 1997, 570–576

trocardiogram was obtained by placing 27 gauge needles subcutaneously in each limb and chest lead. Respiratory rate, cardiac rhythm, and heart rate were continuously monitored during the procedure.

Surgical procedure. The full operative procedure has been previously described (6). In brief, under an operating microscope, the pericardial sac was incised and four epicardial temporary pacing/recording wires were attached to (*a*) the exposed right ventricle; (*b*) the left ventricle; and (*c*) two locations on the right atrial surface. Pacing electrodes are custom-designed stainless steel 0.003 in. Teflon-coated wires (A-M Systems, Inc., Everett, WA). Vascular access was consistently obtained from the right external jugular vein via a cutdown approach. Hemodynamic luminal catheters (0.011 in. internal diameter) were placed antegrade via the jugular vein into the right atrium, with site confirmation by electrogram and pressure tracings.

Electrophysiology study protocol. Unipolar and bipolar electrogram recordings were obtained from right atrium, and right and left ventricular surfaces. Signals were amplified and filtered (EVR recorder; E for M Corp., Lenexa, KS) for oscilloscopic display and thermal paper printout (100 mm/s). Pacing thresholds were determined for each lead and stimulation performed for 1.0 ms pulse widths at twice the diastolic threshold. Bipolar pacing was performed by using a paired unipolar electrode configuration for stimulation from the epicardium (Bloom stimulator; Fischer Imaging Corp., Reading, PA). Cardiac rhythm was continuously monitored, and all ECG intervals (PR, QRS, QT, JT, QTc, RR), axes (P and QRS), and dispersion times were calculated for each animal by a single, experienced observer (CIB) in a blinded, standard fashion (6–8).

Standard clinical electrophysiologic pacing protocols were used to determine all basic electrophysiologic parameters (6, 9–11). The sinus node function was evaluated by measuring sinus node recovery time (SNRT) at two pacing drive rates, including corrected SNRT (SNRT less the sinus cycle length [SCL]) and SNRT/SCL percentage (6, 12). Atrioventricular (A-V) conduction properties were assessed with rapid atrial pacing at rates up to 1,200 bpm. The minimum cycle length maintaining 1:1 A-V conduction, the Wenckebach paced cycle length, and the maximum paced cycle length causing 2:1 A-V block were determined for each animal. Programmed right atrial stimulation was performed to determine atrioventricular and atrial effective refractory periods. Single and double extra-stimulation techniques (down to a minimum coupling interval of 30 ms) were performed to attempt to induce potential atrial arrhythmias. Next, right or left ventricular burst pacing was performed at rates of 250–1,200 bpm to assess retrograde ventriculo-atrial (V-A) conduction, including measurements of V-A Wenckebach block rates, and ventricular pacing exit block. Right and left ventricular effective refractory periods were determined at two paced drive rates using single extrastimuli. Double and triple extrastimulation techniques were then performed to attempt induction of ventricular arrhythmias. Dispersion of refractoriness between the epicardial right and left ventricle sites also was calculated to evaluate any heterogeneity of regional repolarization times.

Pharmacologic effect on basal ECG and electrophysiologic parameters. Analogous to human subjects (9, 13–15), assessment of catecholaminergic effects on cardiac conduction was performed following intravenous infusion of isoproterenol. In mice that were noninducible during the baseline EP study, an isoproterenol infusion (1–10 ng/g per min) was started. As the pharmacokinetics of isoproterenol are not known in mice, the dose was titrated up to attain a 25–30% increase in basal heart rate as in human protocols (9, 11, 15). After several minutes of hemodynamic equilibration, an ECG was

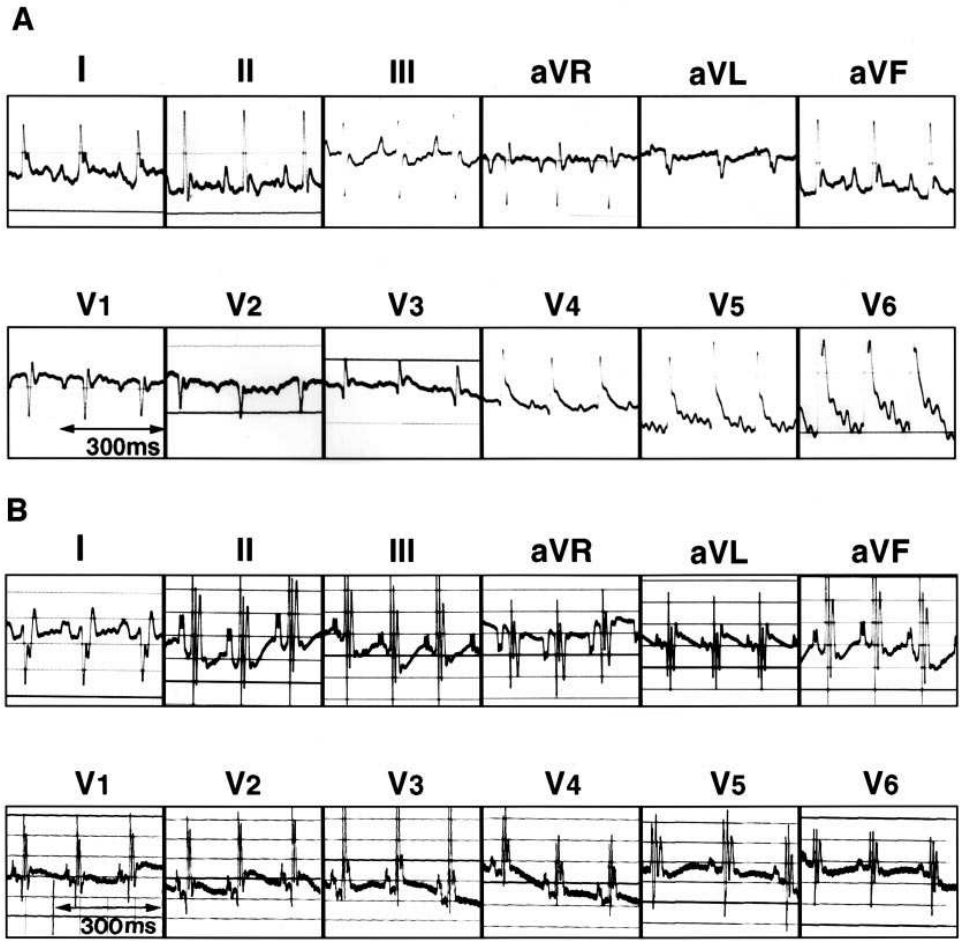

Figure 1. Twelve-lead surface electrocardiograms from wild-type (*A*) and heterozygous $\alpha MHC^{403/+}$ (*B*) mice. In the wild-type mouse ECG, the cycle length is 145 ms (heart rate 414 bpm) with a QRS axis of +45°. In the $\alpha MHC^{403/+}$ mouse ECG, the cycle length is 140 ms (heart rate = 429 bpm) with a QRS axis of +120° and a nonspecific intraventricular conduction abnormality. The paper speed is 75 mm/s and horizontal lines are 1 cm apart (ECG display amplification = 0.1 mV/cm). The low-pass filter is set at 1 Hz and high-pass filter is 50 Hz.

Table I. Electrocardiographic Data Summary

		SCL	HR	PR	QRS	JT	QT	QTc	JTc	QRS axis
			bpm							
Wild type	Mean	120.0	510.8	28.5	18.3	40.8	59.2	171.6	118.7	35.0
	SD	18.4	77.4	5.4	6.2	8.0	10.9	31.2	23.4	68.7
403/+	Mean	128.2	478.9	33.2	20.6	50.5*	71.2*	197.9	140.5	91.8
	SD	21.2	72.5	6.0	4.7	12.4	15.7	30.4	26.3	83.2

All interval values stated in milliseconds. *SCL*, sinus cycle length; *HR*, heart rate; *QTc*, QT/(SCL)$^{1/2}$; *JTc*, JT/(SCL)$^{1/2}$, as defined in (7, 8), **P* value < 0.05.

continuously recorded. The electrophysiologic protocol was then repeated in an identical fashion as in the baseline state to determine catecholamine-dependent changes in arrhythmia inducibility and cardiac conduction properties.

Statistical analysis. All data are presented as the mean±SD. Statistical analyses used the two-tailed Student's *t*-test, with a *P* value of < 0.05 considered significant.

Results

Murine cardiac electrophysiology procedure. A total of 24 mice were evaluated with the mouse EP study protocol (6). Full 12-lead ECG data and right jugular venous access were successfully obtained on all 24 mice (13 control mice, 11 αMHC$^{403/+}$). 18 of the mice completed a full EP study (8 heterozygotes and 10 control mice) with a 75% survival rate. Procedural mortality was related to complications from anesthesia ($n = 1$), mechanical ventilation and intubation ($n = 2$), and cardiac surgical trauma ($n = 3$). The mean age at surgery was 29.9±4 wk in the FHC group and 30.4±4 wk in the control group (P = NS). The mean weight at surgery was 41.6±5 g in the FHC mice and 47.2±6 g in the control mice (P = NS). All studies were performed by investigators fully blinded to mouse genotype.

Electrocardiographic data. Representative surface 12-lead ECG tracings from wild-type and heterozygote αMHC$^{403/+}$ mice are displayed in Fig. 1. ECG parameters for all wild-type and αMHC$^{403/+}$ heterozygote mice studied are shown in Table I. The average resting sinus cycle length was 128±21 ms (heart rate 479±72 bpm) in the FHC mice and 120±18 ms (heart rate 511±77 bpm) in the control mice. The αMHC$^{403/+}$ mice had prolonged ventricular repolarization as measured by the JT and QT intervals on surface ECG (Table I). The mean JT interval in αMHC$^{403/+}$ mice was 50.5±12 ms compared with a mean JT interval of 40.8±8 ms in wild-type mice ($P = 0.03$). The mean QT interval in αMHC$^{403/+}$ mice was 71.2±16 ms vs. 59.2±11 ms in wild-type animals ($P = 0.04$). The QTc and JTc using Bazett's formula (7) were also significantly prolonged in FHC mice ($P < 0.05$ vs. controls).

The FHC mice also exhibited an unusual ECG axis. The QRS frontal plane axis was 92±83° in the FHC group, with 4 of 11 mice exhibiting a QRS axis > 120°. The control group, in comparison, had a mean QRS frontal plane axis of 35±69°,

Table II. Electrophysiologic Data Summary

A. Atrial Pacing Parameters

		SNRT	SCL	CSNRT	SNRT/SCL	AP Wenk	AP 2:1	AVERP100	AERP100
		ms	*ms*	*ms*	%	*ms*	*ms*	*ms*	*ms*
Wild type	Mean	123.6	100.7	22.9	123.2	68.6	55.7	65.7	57.1
	SD	16.5	15.4	9.5	9.9	3.8	5.3	7.9	11.1
403/+	Mean	188.6*	139.0	49.6*	134.9	70.0	58.0	65.0	40.0
	SD	54.2	17.6	46.1	30.1	18.7	14.8	12.9	0.0

B. Ventricular Pacing Parameters

		RV VAC	RV VA Wenk	RV VA 2:1	RVERP100	LV VAC	LV VA Wenk	LV VA 2:1	LVERP100
		Min ms	*ms*	*ms*	*ms*	*Min ms*	*ms*	*ms*	*ms*
Wild type	Mean	80.0	70.0	55.0	58.0	76.0	66.0	55.0	56.0
	SD	11.5	11.5	10.8	12.3	5.2	5.2	5.3	8.4
403/+	Mean	83.8	74.4	61.3	62.5	83.8*	75.0*	63.8*	67.5*
	SD	14.1	12.9	14.6	19.8	7.4	7.1	11.9	12.8

The atrial pacing capture thresholds were 0.24±0.10 mA in both groups. Ventricular pacing capture thresholds were 0.13±0.07 mAmperes in the FHC group and 0.12±0.06 mAmperes in the control group. All interval values are in milliseconds. A-V conduction was assessed by rapid right atrial pacing down to cycle lengths as short as 40 ms (i.e. pacing rate = 1500 bpm). The αMHC$^{403/+}$ mice had 1:1 A-V conduction down to a mean paced cycle length of 80±18 ms, with Wenckebach-type periodicity at a mean paced cycle length of 70±19 and 2:1 A-V block with more rapid pacing at a mean of 58±14 ms. The control animals, similarly, demonstrated 1:1 A-V conduction to 78±4 ms, Wenckebach block at 69±4 ms, and 2:1 A-V block at 56±5 ms (P = not significant). *SNRT*, sinus node recovery time; *SCL*, sinus cycle length; *CSNRT*, corrected sinus node recovery time (=SNRT-SCL); *AP Wenk*, atrial pacing Wenckebach cycle length; *AP 2:1*, atrial pacing 2:1 atrioventricular block cycle length; *AVERP*, atrioventricular (and/or His-Purkinje system) effective refractory period; *AERP*, atrial effective refractory period; *VAC min CL*, ventriculo-atrial conduction minimum cycle length; *VA Wenk*, ventricular paced maximum cycle length allowing ventriculo-atrial conduction; *VA 2:1*, ventricular paced minimum cycle length causing 2:1 ventriculo-atrial block; *VP*, ventricular pacing; *VERP*, ventricular effective refractory period; *RV*, right ventricle; *LV*, left ventricle; **P* value < 0.05.

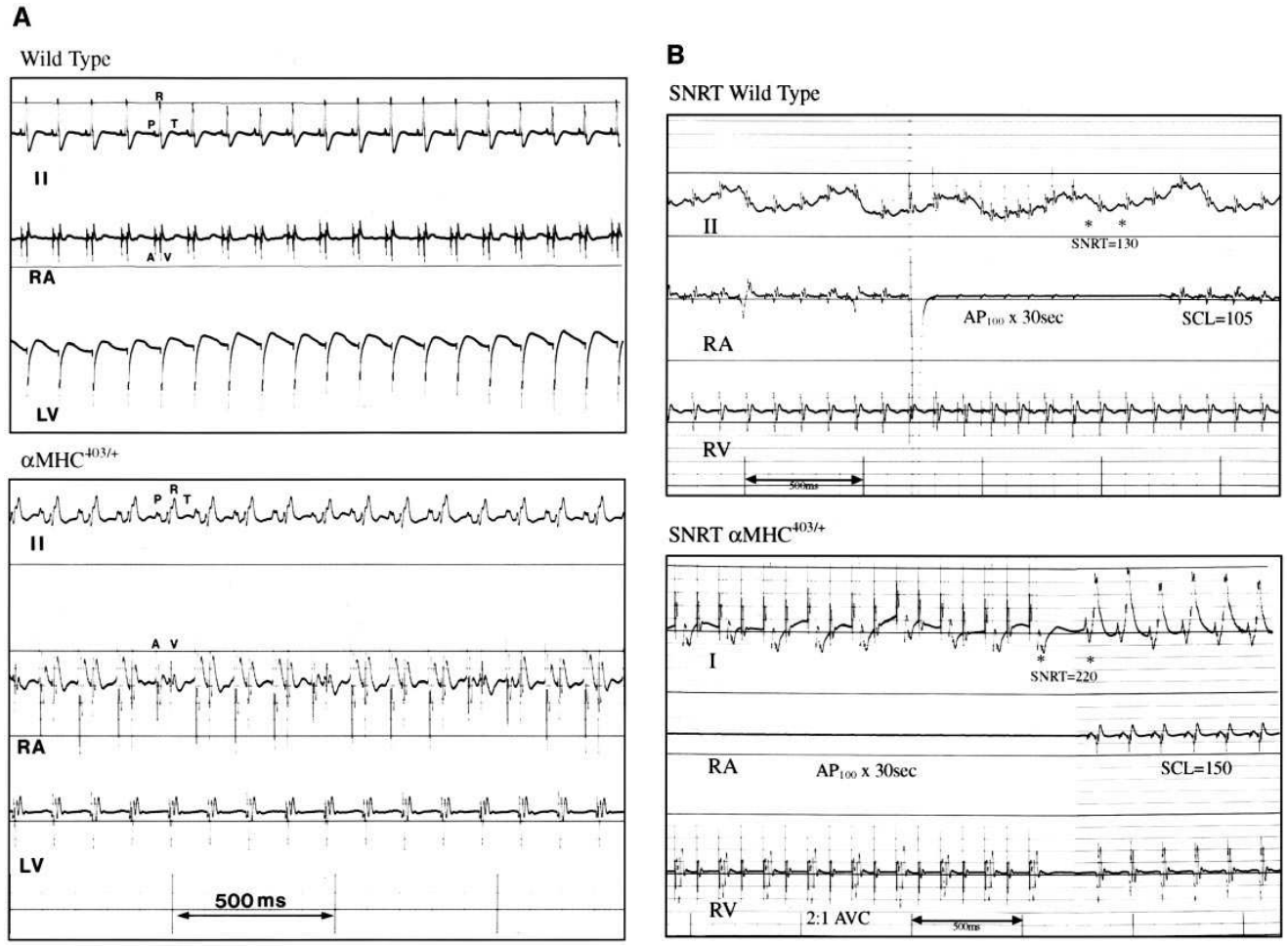

Figure 2. (*A*) Three-channel recordings during normal sinus rhythm from wild-type (*top*) and αMHC$^{403/+}$ mice (*bottom*). The surface ECG lead II and intracardiac bipolar electrograms from right atrium (*RA*) and left ventricle (*LV*) are shown. On the surface lead, P, R, and T waves are marked during one cardiac cycle. On the atrial electrogram, both an atrial (*A*) and ventricular (*V*) deflection are inscribed. The electrograms from the αMHC$^{403/+}$ mouse are notable for being markedly fractionated. Paper speed is 100 mm/s, vertical calibration lines are 100 ms markers and horizontal lines are one cm apart (ECG display amplification = 0.1 mV/cm). Surface ECG filters were set between 1 and 50 Hz, and intracardiac electrogram filters were set between 10 and 250 Hz. (*B*) Sinus node recovery time (*SNRT*) from wild-type (*top*) and αMHC$^{403/+}$ (*bottom*) mice. A surface ECG lead and intracardiac right atrial (*RA*) and right ventricular (*RV*) bipolar electrograms are displayed. A time break was introduced in the figure during the 30 s of atrial pacing to allow both pacing and SNRT to be shown on the same figure. After 30 s of rapid atrial pacing at 100 ms (AP_{100}), the SNRT is measured from the last paced atrial beat (*first asterisk*) to the first sinus return beat (*second asterisk*), corrected for the sinus cycle length (*SCL*). In the wild-type, the corrected sinus node recovery time (CSNRT=SNRT-SCL) is 130–105 = 25 ms. In the αMHC$^{403/+}$ mouse, during rapid atrial pacing at 100 ms (AP_{100}), there is 2:1 atrioventricular conduction (2:1 AVC) demonstrated on both the surface ECG and RV electrogram, and following atrial pacing, the CSNRT = 220–150 = 70 ms.

and no control mouse (0/13) had an axis ≥ 120° on ECG ($P <$ 0.05, FHC vs. control).

Cardiac conduction properties and electrophysiological data. Atrial, atrioventricular, and ventricular conduction properties were all assessed in wild-type and αMHC$^{403/+}$ mice. Sinus node function was evaluated by measuring the rate-corrected sinus node recovery time (CSNRT) (12). Representative three-channel recordings of surface, atrial, and ventricular intracardiac electrograms for wild-type and αMHC$^{403/+}$ mice are shown in Fig. 2. A significant difference in sinus node function between the wild-type and the FHC mice was detected. In control animals, the CSNRT ranged between 10 and 30 ms, with a mean of 22.9±9 ms. In the FHC heterozygotes, the CSNRT ranged from 22 to 150 ms, with a mean of 47.8±50 ms. Three of the eight FHC mice studied had a CSNRT > 30 ms ($P < 0.05$). The atrial, atrioventricular, and right ventricular effective refractory periods (RV ERP) were not significantly different between the αMHC$^{403/+}$ heterozygote and control groups. The left ventricular (LV) conduction properties, however, were significantly slower in the FHC mice, while RV conduction appeared similar to that seen in the wild-type mice (Table II). During incremental rapid LV pacing, retrograde ventriculoatrial (VA) conduction was blocked earlier in the pacing protocol (75±7 ms) in FHC mice than in control mice (66±5 ms; $P < 0.01$). LV 2:1 VA block occurred at 64±12 ms in the FHC group versus 55±5 ms in the controls ($P < 0.05$). Finally, the left ventricular effective refractory period (LV ERP) was prolonged to 67±13 ms in FHC mice versus 56±8 ms in controls ($P < 0.05$). These differences were not evident when identical pacing protocols were performed from the RV

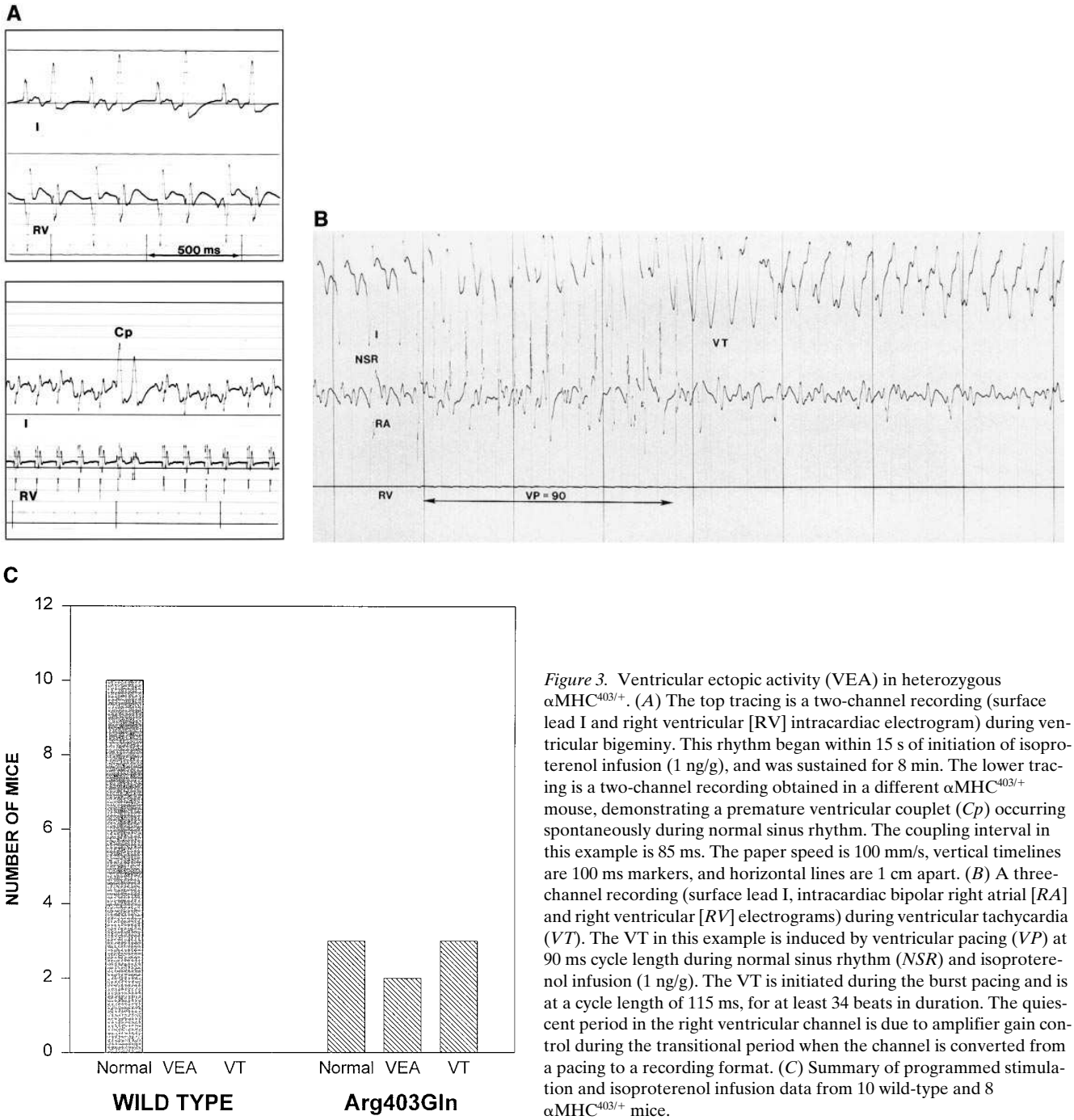

Figure 3. Ventricular ectopic activity (VEA) in heterozygous $\alpha MHC^{403/+}$. (*A*) The top tracing is a two-channel recording (surface lead I and right ventricular [RV] intracardiac electrogram) during ventricular bigeminy. This rhythm began within 15 s of initiation of isoproterenol infusion (1 ng/g), and was sustained for 8 min. The lower tracing is a two-channel recording obtained in a different $\alpha MHC^{403/+}$ mouse, demonstrating a premature ventricular couplet (*Cp*) occurring spontaneously during normal sinus rhythm. The coupling interval in this example is 85 ms. The paper speed is 100 mm/s, vertical timelines are 100 ms markers, and horizontal lines are 1 cm apart. (*B*) A three-channel recording (surface lead I, intracardiac bipolar right atrial [*RA*] and right ventricular [*RV*] electrograms) during ventricular tachycardia (*VT*). The VT in this example is induced by ventricular pacing (*VP*) at 90 ms cycle length during normal sinus rhythm (*NSR*) and isoproterenol infusion (1 ng/g). The VT is initiated during the burst pacing and is at a cycle length of 115 ms, for at least 34 beats in duration. The quiescent period in the right ventricular channel is due to amplifier gain control during the transitional period when the channel is converted from a pacing to a recording format. (*C*) Summary of programmed stimulation and isoproterenol infusion data from 10 wild-type and 8 $\alpha MHC^{403/+}$ mice.

electrodes. Interestingly, five of the eight FHC mice displayed markedly fractionated electrograms (cf. Fig. 2), compared to 2 of the 10 wild-type mice. Such fractionation of the ventricular electrogram also has been seen in association with ventricular tachycardia in human FHC patients (16).

Programmed stimulation and arrhythmia inducibility. Using standard programmed electrical stimulation protocols and burst atrial and ventricular pacing, provocation of ectopic or reentrant rhythms was attempted (9, 17). As in human EP protocols, if no arrhythmia is induced following the full murine EP protocol, an intravenous infusion of isoproterenol (1–10 ng/g per min) is instituted via a central venous catheter and is titrated to an increase in basal heart rate of 20–30% to accelerate conduction properties and provoke catecholamine-sensitive tachyarrhythmias (6, 9). None of the wild-type or $\alpha MHC^{403/+}$ mice had atrial arrhythmias, either at baseline or with isoproterenol provocation. Additionally, none of the 10 wild-type mice had any inducible ventricular ectopic activity with programmed stimulation. Eight of these wild-type mice also received an isoproterenol infusion (mean dose 5±2 ng/g per min) with a mean increase in heart rate of 25% (decrease in cycle length from 120±18 ms to 91±14 ms), but none had isoproterenol-provoked ventricular arrhythmia. In contrast with the wild-type controls, ventricular ectopy was inducible reproducibly in five of the eight $\alpha MHC^{403/+}$ mice studied (Fig. 3). Ventricular ectopy occurred spontaneously or was provoked

by programmed stimulation alone in three of the FHC mice, and with isoproterenol infusion and stimulation in another two mice. In all cases, burst ventricular pacing involved stimulation of 10–20 beats at a cycle length between 150 and 50 ms or use of double or triple ventricular premature beats. Ventricular ectopy was reproduced with repeat pacing between two and five times in these mice. As with the wild-type mice, isoproterenol (mean dose 3±2 ng/g per min) increased the heart rate by 23% in the FHC mice (decrease in cycle length from 128±21 to 98±9 ms). Two $\alpha MHC^{403/+}$ mice had frequent ventricular ectopy, including bigeminal rhythm and ventricular couplets or triplets (Fig. 3 *A*). Three other $\alpha MHC^{403/+}$ mice had nonsustained or sustained ventricular tachycardia (Fig. 3 *B*).

Discussion

The experiments presented here identify several electrophysiologic differences between the heterozygous $\alpha MHC^{403/+}$ mutant mice and their wild-type littermates. The FHC mice displayed surface ECG abnormalities including prolonged repolarization times (JT, QT, JTc, QTc), however, specific differences in interlead QT and JT dispersion could not be determined due to difficulty in identifying the T-wave offset in multiple ECG leads. Right axis deviation > 120° was seen on the surface ECG in 36% of FHC mice studied, which may be due to abnormal cardiac morphology or to left posterior hemiblock (18). There was no obvious evidence for RV hypertrophy, pulmonary hypertension, or RV outflow obstruction as potential hemodynamic explanations for the right axis deviation. The FHC mice also had distinct EP abnormalities, including differential conduction properties between the LV and RV, which were not evident in wild-type controls. LV pacing abnormalities including prolonged ventricular repolarization and increased electrogram fractionation also were observed, and may be factors in arrhythmia vulnerability in the mice. In addition, the $\alpha MHC^{403/+}$ mice had prolonged CSNRTs which were consistent with either intrinsic sinus node dysfunction, or perhaps secondary to autonomic derangements due to altered hemodynamics. Finally, the majority of the $\alpha MHC^{403/+}$ mice evaluated had inducible ventricular ectopic activity (Fig. 3), which was not observed in any of the wild-type mice. Four of the five $\alpha MHC^{403/+}$ mice with fractionated ventricular electrograms also had inducible ventricular ectopy. Interestingly, three of the eight $\alpha MHC^{403/+}$ mice had no inducible arrhythmia, and those with arrhythmias had variable degrees of ventricular ectopic activity, ranging from bigeminy to sustained polymorphic ventricular tachycardia. While the molecular mechanism responsible for such variability is not yet clear, this range of electrophysiologic abnormalities in the FHC mice may be related to the variability in myocardial histopathology noted previously in these mice (5). It is not yet clear, however, whether the severity of the histopathology or hemodynamic derangements in these mice correlates with electrophysiological abnormalities or with arrhythmia vulnerability. Studies to examine these possibilities are in progress. Additionally, it is possible that the FHC mice may have more pronounced autonomic responses to surgery and/or anesthesia, which could contribute to primary hemodynamic derangements with secondary electrical dysfunction. Finally, this study does not directly address whether the inducible ventricular arrhythmias seen in the FHC mice are responsible for or contribute to the exercise-provoked sudden death noted previously in these animals, though it provides a new potential explanation for the sudden death observed in these mutant mice (5).

The familial hypertrophic cardiomyopathies are characterized by ventricular hypertrophy with associated myocyte disarray, myocardial interstitial fibrosis, and ventricular arrhythmias. Thus far, the abnormal genes identified in humans with FHC encode for mutations in sarcomeric proteins, such as α- and β-myosin heavy chain, α-tropomyosin, and cardiac troponin T (4, 19, 20). The clinical course of FHC is highly variable, with a spectrum at presentation that ranges from the asymptomatic carrier state to premature sudden death in childhood. The risk factors for sudden death in FHC include young age at presentation, syncope, myocardial ischemia, inducible sustained ventricular tachycardia during EP study, and a malignant family history (21–24). In FHC patients who have survived cardiac arrest, electrophysiologic testing has demonstrated that sinus node dysfunction, electrogram fractionation, and inducible ventricular arrhythmias are common (16, 25, 26). Specific mutations causing FHC are associated in some patients with echocardiographic evidence for ventricular hypertrophy and morphological abnormalities (27), risk for sudden death and/or ventricular arrhythmias (28), and electrophysiological abnormalities (29, 30). Current diagnostic techniques, however, such as echocardiography and cardiac catheterization, are neither sensitive nor specific predictors of sudden death in patients with familial hypertrophic cardiomyopathy. Clinical electrophysiological testing has had variable predictive value in these patients, in part because it has not been possible to study the electrophysiologic abnormalities associated with a specific genotype in human cohorts (3, 31).

The studies in this report demonstrate a new approach to examining directly the relationship between a specific genotype and its electrophysiologic phenotype. The $\alpha MHC^{403/+}$ mutation studied here is associated in humans with a relatively high risk of arrhythmia and mortality (28). These data identify specific electrophysiological abnormalities associated with the $\alpha MHC^{403/+}$ mutation and raise the possibility that prospective evaluation of ECG and EP parameters (e.g., ECG axis, CSNRT) and arrhythmia inducibility may be of value in predicting which patients with FHC due to the corresponding Arg403Gln mutation are at risk for electrophysiologic sequelae and sudden death. In addition, the present study provides an approach to general evaluation of EP abnormalities associated with specific genetic diseases. Determination of specific electrophysiological abnormalities associated with other mutations that cause FHC, and with other genetic disorders, may be explored in this manner. Furthermore, potential therapies for FHC and other genetic diseases with electrophysiologic phenotypes may be evaluated in electrophysiologic studies of mutant mice. Such studies may include assessment of existing and investigational anti-arrhythmic drugs or therapeutic pacing modalities, and specific gene therapy approaches. Study of cardiac electrophysiology in transgenic mouse models thus will be of value in the development of both diagnostic and therapeutic approaches to human disease.

Acknowledgments

The authors gratefully acknowledge David Fulton and Mark Estes for helpful discussions. We are grateful to Patricia Nayak for expert preparation of the manuscript.

This work was supported in part by an Institutional Research

Grant from New England Medical Center and by NIH Clinical Investigator Development Award HL03607 to C.I. Berul. M.E. Mendelsohn is an Established Investigator of the American Heart Association.

References

1. Paigen, K. 1995. A miracle enough: the power of mice. *Nat. Med.* 1:215–220.

2. Lin, M.C., R.A. Rockman, and K.R. Chien. 1995. Heart and lung disease in engineered mice. *Nat. Med.* 1:749–751.

3. Seidman, C.E., and J.G. Seidman. 1995. Gene mutations that cause familial hypertrophic cardiomyopathy. *In* Molecular Cardiovascular Medicine. E. Haber, editor. Scientific American Press, New York. 193–210.

4. Watkins, H., W. McKenna, L. Thierfelder, H.J. Suk, R. Anan, A. O'Donoghue, P. Spirito, A. Matsumori, C.S. Moravec, J.G. Seidman, and C.E. Seidman. 1995. Mutations in the genes for cardiac troponin T and α-tropomyosin in hypertrophic cardiomyopathy. *N. Engl. J. Med.* 332:1058–1064.

5. Geisterfer-Lowrance, A., M. Christe, D. Conner, J. Ingwall, F. Schoen, C.E. Seidman, and J.G. Seidman. 1996. A mouse model of familial hypertrophic cardiomyopathy. *Science (Wash. DC).* 272:731–734.

6. Berul, C.I., M. Aronovitz, P.J. Wang, and M.E. Mendelsohn. 1996. In vivo cardiac electrophysiology studies in the mouse. *Circulation.* 94:2641–2648.

7. Bazett, H.C. 1920. An analysis of the time relationships of the heart. *Heart.* 7:353–370.

8. Berul, C.I., T.L. Sweeten, A.M. Dubin, M.J. Shah, and V.L. Vetter. 1994. Use of the rate-corrected JT interval for prediction of repolarization abnormalities in children. *Am. J. Cardiol.* 74:1254–1257.

9. Gillette, P.C., D.S. Buckles, M. Harold, and A. Garson. 1990. Intracardiac electrophysiology studies. *In* Pediatric Arrhythmias: Electrophysiology and Pacing. P.C. Gillette and A. Garson, editors. W.B. Saunders, Philadelphia. 216–248.

10. Roberts, N.K., and P.C. Gillette. 1977. Electrophysiologic study of the conduction system in normal children. *Pediatrics.* 60:858–863.

11. Kugler, J.D. 1995. Electrophysiology studies. *In* Moss and Adam's Heart Disease in Infants, Children, and Adolescents, Including the Fetus and Young Adult. G.C. Emmanouilides, T.A. Reimenschneider, H.D. Allen, and H.P. Gutgesell, editors. Williams & Wilkins, Baltimore. 347–366.

12. Mandel, W., H. Hayakawa, R. Danzig, and H.S. Marcus. 1971. Evaluation of sino-atrial node function in man by overdrive suppression. *Circulation.* 44:59–66.

13. Randall, W.C. 1990. Sympathetic modulation of normal cardiac rhythm. *In* Cardiac Electrophysiology: A Textbook. M.R. Rosen, M.J. Janse, and A.L. Wit, editors. Futura, Mount Kisko, NY. 889–901.

14. Wit, A.L., M.B. Weiss, and W.D. Berkowitz. 1970. Patterns of A-V conduction in the human heart. *Circ. Res.* 27:345–352.

15. Zipes, D.P. 1992. Specific arrhythmias: diagnosis and treatment. *In* Heart Disease: A Textbook of Cardiovascular Medicine. E. Braunwald, editor. W.B. Saunders, Philadelphia. 667–725.

16. Watson, R.M., J.L. Schwartz, B.J. Maron, E. Tucker, D.R. Rosing, and M.E. Josephson. 1987. Inducible polymorphic ventricular tachycardia and ventricular fibrillation in a subgroup of patients with hypertrophic cardiomyopathy at risk for sudden death. *J. Am. Coll. Cardiol.* 10:761–774.

17. Vetter, V.L. 1985. The pediatric electrophysiology study. *In* Pediatric and Fundamental Electrocardiography. J. Liebman, R. Plonsey, and Y. Rudy, editors. Martinus Nijhoff, New York. 161–184.

18. Scheidt, S. 1984. Basic electrocardiography: abnormalities of electrocardiographic patterns. *Clinical Symposia.* 36:2–32.

19. Thierfelder, L., H. Watkins, C. MacRae, R. Lamas, W. McKenna, H.P. Vosberg, J.G. Seidman, and C.E. Seidman. 1994. Mutations in α-tropomyosin and in cardiac troponin T cause hypertrophic cardiomyopathy: a disease of the sarcomere. *Cell.* 77:701–712.

20. Watkins, H., R. Anan, D.A. Coviello, P. Spirito, J.G. Seidman, and C.E. Seidman. 1995. A *de novo* mutation in α-tropomyosin that causes hypertrophic cardiomyopathy. *Circulation.* 91:2302–2305.

21. Fananapazir, L., A.C. Chang, S.E. Epstein, and D. McAreavy. 1992. Prognostic determinants in hypertrophic cardiomyopathy: prospective evaluation of a therapeutic strategy based on clinical, holter, hemodynamic, and electrophysiological findings. *Circulation.* 86:730–740.

22. Epstein, N.D., G.M. Cohn, F. Cyran, and L. Fananapazir. 1992. Differences in clinical expression of hypertrophic cardiomyopathy associated with two distinct mutations in β-myosin heavy chain gene. *Circulation.* 86:345–352.

23. Buja, G., M. Miorelli, P. Turrini, P. Melacini, and A. Nava. 1993. Comparison of QT dispersion in hypertrophic cardiomyopathy between patients with and without ventricular arrhythmias and sudden death. *Am. J. Cardiol.* 72: 973–976.

24. Wigle, E.D., H. Rakowski, B.P. Kimball, and W.G. Williams. 1995. Hypertrophic cardiomyopathy: clinical spectrum and treatment. *Circulation.* 92: 1680–1692.

25. Fananapazir, L., and S.E. Epstein. 1991. Hemodynamic and electrophysiologic evaluation of patients with hypertrophic cardiomyopathy surviving cardiac arrest. *Am. J. Cardiol.* 67:280–287.

26. Maron, B.J., and L. Fananapazir. 1992. Sudden cardiac death in hypertrophic cardiomyopathy. *Circulation.* 85:I57–I63.

27. Solomon, S.D., S. Wolff, H. Watkins, P.M. Ridker, P. Come, W.J. McKenna, C.E. Seidman, and R.T. Lee. 1993. Left ventricular hypertrophy and morphology in familial hypertrophic cardiomyopathy associated with mutations of the beta-myosin heavy chain gene. *J. Am. Coll. Cardiol.* 22:498–505.

28. Watkins, H., A. Rosenzweig, D. Hwang, T. Levi, W. McKenna, C.E. Seidman, and J.G. Seidman. 1992. Characteristics and prognostic implications of myosin missense mutations in familial hypertrophic cardiomyopathy. *N. Engl. J. Med.* 326:1108–1114.

29. Spirito, P., C. Rapezzi, C. Autore, P. Bruzzi, P. Bellone, P. Ortolani, P.V. Fragola, F. Chiarella, M. Zoni-Berisso, A. Branzi, et al. 1994. Prognosis of asymptomatic patients with hypertrophic cardiomyopathy and nonsustained ventricular tachycardia. *Circulation.* 90:2743–2747.

30. McKenna, W.J., N. Sadoul, A.K.B. Slade, and R.C. Saumarez. 1994. The prognostic significance of nonsustained ventricular tachycardia in hypertrophic cardiomyopathy. *Circulation.* 90:3115–3117.

31. Cannon, C.R., G.S. Reeder, K.R. Bailey, L.J. Melton III, and B.J. Gersh. 1995. Natural history of hypertrophic cardiomyopathy: a population-based study, 1976 through 1990. *Circulation.* 92:2488–2495.